

# Optomechanically induced nonreciprocity in a three-mode optomechanical system

Xun-Wei Xu,<sup>1,\*</sup> L. N. Song,<sup>2</sup> Qiang Zheng,<sup>3,2</sup> Z. H. Wang,<sup>4,2</sup> and Yong Li<sup>2,†</sup>

<sup>1</sup>*Department of Applied Physics, East China Jiaotong University, Nanchang, 330013, China*

<sup>2</sup>*Beijing Computational Science Research Center, Beijing 100193, China*

<sup>3</sup>*School of Mathematics, Guizhou Normal University, Guiyang, 550001, China*

<sup>4</sup>*Center for Quantum Sciences and School of Physics, Northeast Normal University, Changchun 130024, China*

(Dated: January 1, 2019)

We propose to create optical nonreciprocity in a three-mode optomechanical system comprising one mechanical and two optical modes, where the mechanical mode is coupled with only one of the optical modes. The optical nonreciprocal response of the system is based on the nonlinearity induced by the optomechanical interaction. However, nonlinearity is a necessary but not a sufficient condition for observing nonreciprocity. Another necessary condition for nonreciprocal response of the system to a classical driving field is demonstrated analytically. The effects of the parameters on the nonreciprocal response of the system are discussed numerically. The three-mode optomechanical system provides a platform to realize nonreciprocity for strong optical signal fields.

## I. INTRODUCTION

Optomechanical system with parameter coupling between optical and mechanical modes provides us a perfect platform for various classical and quantum information processing applications [1–6]. As an important application, the design of nonreciprocal devices, that allow signals transmitting in one direction while blocking those propagating in the opposite one, based on optomechanical interaction has attracted significant interest in the past few years [7, 8]. A number of designs based on diverse mechanisms are proposed to demonstrate nonreciprocity in optomechanical systems. As a non-magnetic scheme, optomechanically induced nonreciprocity makes the all-optical controllable isolators and circulators integrated on chip easily.

Optomechanically induced transparency (OMIT) is a phenomenon that a tunable transparent window for a weak probe is induced by the optomechanical coupling with a strong driving field injected into the red-detuned sideband of an optomechanical system [9–13]. OMIT in microring resonators provides us a practical way to achieve optical nonreciprocity [14]. The symmetry for the transmission of weak signals is broken in the presence of a strong driving field. Specifically, a strong driving field in the red sideband of the system induces a transparent transmission window for signals propagating in the same direction as the driving field, but not in the opposite one, leading to optical isolation, which has already been observed in experiments [15, 16]. Similar to the OMIT, stimulated Brillouin scattering (SBS) between two optical modes by a travelling acoustic mode can also induce transparency when they satisfy both the energy and momentum conservations, and has been used successfully for the generation of nonreciprocity in optomechanical systems [17, 18].

Besides the optomechanical nonreciprocity in degenerate whispering-gallery modes with inherent non-trivial topology, the nonreciprocity via synthetic magnetism and reservoir engineering has been proposed theoretically [19–24] and real-

ized experimentally in an optomechanical circuit [25–28]. The time-reversal symmetry is broken by a synthetic magnetic flux by phase-correlated driving fields, which may enhance the photonic transport in one direction for constructive quantum interference but suppress it in the reversal direction due to destructive quantum interference.

Another approach to create nonreciprocity in the optomechanical system is by using the Kerr-type nonlinear interaction induced by the mechanical mode. As early as in 2009, the nonreciprocal optical transmission spectrum has been demonstrated in a Fabry-Perot cavity with one movable mirror by the asymmetry of the radiation pressure on the movable mirror for forward and backward incident light [29]. Moreover, the optical nonreciprocity was also proposed in optomechanical systems with asymmetric structures [30, 31].

However, there are substantial differences between the nonreciprocity based on nonlinearity and the ones based on the other mechanisms mentioned above (e.g., OMIT, SBS, and synthetic magnetic flux). For the nonreciprocity based on nonlinearity, there is only one light beam injected into the optomechanical system and the structure is nonreciprocal for this light, which is usually pretty strong. Instead, the nonreciprocity based on the other mechanisms is nonreciprocal for a weak light beam (signal field) in the presence of a strong light beam (control field). When the signal field is strong, the nonreciprocity based on nonlinearity would be a better choice.

In this paper, we propose the creation of optical nonreciprocity in a three-mode optomechanical system based on the optomechanical induced nonlinearity [29–31]. Different from the previous works [29–31], here the setup consists of one mechanical and two optical (cavity) modes, and the mechanical mode is coupled with only one of the optical modes. Interestingly, we find that the nonlinearity is a necessary but not a sufficient condition for observing nonreciprocity. Another condition is necessary for creating the nonreciprocal response of the system to the classical driving field. The effects of the parameters on the nonreciprocal response of the system are discussed numerically.

The remainder of this paper is organized as follows. In Sec. II, we introduce the theoretical model of three-mode optomechanical system, and derive the nonlinear equations for the output fields. In Sec. III, the nonreciprocal responses of

\*Electronic address: [davidxu0816@163.com](mailto:davidxu0816@163.com)

†Electronic address: [liyong@csrc.ac.cn](mailto:liyong@csrc.ac.cn)

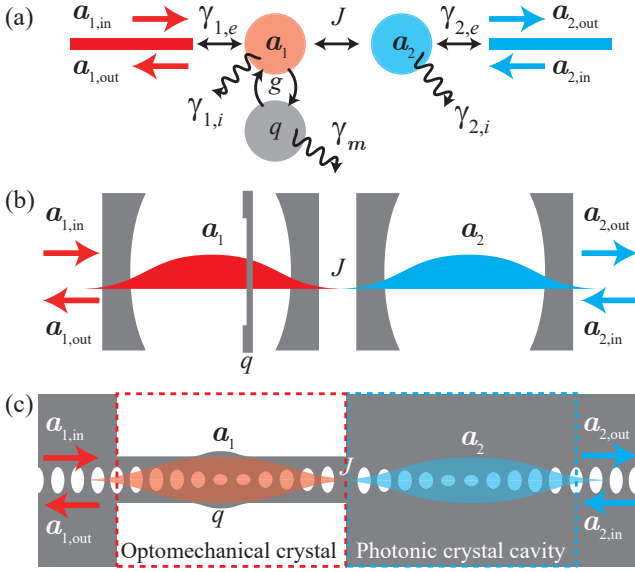


FIG. 1: (Color online) (a) Scheme of a three-mode optomechanical system consisting of two linearly coupled optical modes ( $a_1$  and  $a_2$ ) and a mechanical mode ( $q$ ) coupled to one of the optical modes via optomechanical interaction. (b) and (c) Example implementations of the three-mode optomechanical system: (b) a membrane in the middle of one of the two coupled optical cavities [33–36], and (d) an optomechanical crystal coupled to the photonic crystal cavity [25, 32].

the system to the classical driving field are discussed numerically. Finally, a summary is given in Sec. IV.

## II. THEORETICAL MODEL

We consider an optomechanical system consisting of two linearly coupled optical modes ( $a_1$  and  $a_2$ , with frequencies  $\omega_1$  and  $\omega_2$ ) and one of them is coupled to a mechanical mode ( $p$  and  $q$ , with vibrational frequency  $\omega_m$ ) through optomechanical interaction, as shown in Fig. 1(a), that is described by the Hamiltonian ( $\hbar = 1$ )

$$\begin{aligned}
 H = & \omega_1 a_1^\dagger a_1 + \omega_2 a_2^\dagger a_2 + \frac{1}{2} \omega_m (q^2 + p^2) \\
 & + J (a_1^\dagger a_2 + a_2^\dagger a_1) + g a_1^\dagger a_1 q \\
 & + i \sqrt{\eta_1 \gamma_1} (a_1^\dagger a_{1,\text{in}} e^{-i\omega_1 t} - a_1 a_{1,\text{in}}^\dagger e^{i\omega_1 t}) \\
 & + i \sqrt{\eta_2 \gamma_2} (a_2^\dagger a_{2,\text{in}} e^{-i\omega_2 t} - a_2 a_{2,\text{in}}^\dagger e^{i\omega_2 t}). \quad (1)
 \end{aligned}$$

Here  $J$  is the coupling strength between the two optical modes and  $g$  denotes the single-photon optomechanical coupling strength. We assume that  $\gamma_j = \gamma_{j,i} + \gamma_{j,e}$  ( $j = 1, 2$ ) is the total decay rate of the optical mode  $a_j$  with the cavity coupling parameter  $\eta_j = \gamma_{j,e}/(\gamma_{j,i} + \gamma_{j,e})$ , where  $\gamma_{j,i}$  denotes the intrinsic decay rate and  $\gamma_{j,e}$  the external decay rate (i.e. waveguide-to-cavity coupling).  $a_{j,\text{in}}$  and  $\omega_d$  are the driving amplitude and frequency at the input of the optical mode  $a_j$  via the waveguide-to-cavity coupling  $\gamma_{j,e} = \eta_j \gamma_j$ . Such a system can be implemented in two linearly coupled Fabry-Pérot

cavities with a membrane in the node of one of the optical cavities [see Fig. 1(b)] [33–36], and an optomechanical crystal coupled to the photonic crystal cavity [see Fig. 1(c)] [25, 32].

In the rotating frame of the driving frequency  $\omega_d$ , the dynamics of the system is described by the quantum Langevin equations (QLEs)

$$\begin{aligned}
 \frac{d}{dt} a_1 = & - \left( \frac{\gamma_1}{2} + i \Delta_1 \right) a_1 - ig q a_1 - i J a_2 \\
 & + \sqrt{\eta_1 \gamma_1} a_{1,\text{in}} + \sqrt{(1 - \eta_1) \gamma_1} a_{1,\text{vac}}, \quad (2)
 \end{aligned}$$

$$\begin{aligned}
 \frac{d}{dt} a_2 = & - \left( \frac{\gamma_2}{2} + i \Delta_2 \right) a_2 - i J a_1 \\
 & + \sqrt{\eta_2 \gamma_2} a_{2,\text{in}} + \sqrt{(1 - \eta_2) \gamma_2} a_{2,\text{vac}}, \quad (3)
 \end{aligned}$$

$$\frac{d}{dt} q = \omega_m p, \quad (4)$$

$$\frac{d}{dt} p = -\omega_m q - g a_1^\dagger a_1 - \gamma_m p + \xi, \quad (5)$$

where  $\Delta_j = \omega_j - \omega_d$  is the detuning parameter,  $\gamma_m$  is the decay rate of the mechanical mode;  $a_{1,\text{vac}}$ ,  $a_{2,\text{vac}}$ , and  $\xi$  are the input quantum noise operators with zero mean values,  $\langle a_{1,\text{vac}} \rangle = 0$ ,  $\langle a_{2,\text{vac}} \rangle = 0$ ,  $\langle \xi \rangle = 0$ .

Each operator of the optical and mechanical modes can be split into a classical mean value and fluctuation:  $a_j = \alpha_j + \delta a_j$ ,  $a_{j,\text{in}} = \alpha_{j,\text{in}} + \delta a_{j,\text{in}}$ ,  $q = \bar{q} + \delta q$ ,  $p = \bar{p} + \delta p$ , with the ansatz  $\alpha_j = \langle a_j \rangle$ ,  $\alpha_{j,\text{in}} = \langle a_{j,\text{in}} \rangle$ ,  $\bar{q} = \langle q \rangle$ ,  $\bar{p} = \langle p \rangle$ . Under the condition of strong driving and weak optomechanical coupling, i.e.,  $\sqrt{\eta_j \gamma_j} |\alpha_{j,\text{in}}| \gg \gamma_j \gg g$ , the classical mean values and quantum fluctuations can be treated separately. In the steady state for  $d\alpha_i/dt = 0$  and  $d\bar{p}/dt = d\bar{q}/dt = 0$ , the mean values ( $\alpha_i, \bar{q}$ ) are given by

$$0 = - \left( \frac{\gamma_1}{2} + i \Delta_1 \right) \alpha_1 - ig \bar{q} \alpha_1 - i J \alpha_2 + \sqrt{\eta_1 \gamma_1} \alpha_{1,\text{in}}, \quad (6)$$

$$0 = - \left( \frac{\gamma_2}{2} + i \Delta_2 \right) \alpha_2 - i J \alpha_1 + \sqrt{\eta_2 \gamma_2} \alpha_{2,\text{in}}, \quad (7)$$

$$\omega_m \bar{q} = -g |\alpha_1|^2, \quad (8)$$

where the mean-field approximation (e.g.,  $\langle q a_1 \rangle \approx \langle q \rangle \langle a_1 \rangle$ ) is used in the derivation. By introducing the vectors  $f = (\delta a_1 \ \delta a_1^\dagger \ \delta a_2 \ \delta a_2^\dagger \ \delta q \ \delta p)^T$  and  $\zeta = (\delta A_{1,\text{in}} \ \delta A_{1,\text{in}}^\dagger \ \delta A_{2,\text{in}} \ \delta A_{2,\text{in}}^\dagger \ 0 \ \xi)$ , with  $\delta A_{j,\text{in}} = \sqrt{\eta_j \gamma_j} \delta a_{j,\text{in}} + \sqrt{(1 - \eta_j) \gamma_j} a_{j,\text{vac}}$ , the linearized QLEs for the fluctuation operators of the optical and mechanical modes can be given in the matrix form as

$$\frac{d}{dt} f = A f + \zeta, \quad (9)$$

where the coefficient matrix

$$A = \begin{pmatrix} -\left(\frac{\gamma_1}{2} + i\Delta'_1\right) & 0 & -iJ & 0 & -ig\alpha_1 & 0 \\ 0 & -\left(\frac{\gamma_1}{2} - i\Delta'_1\right) & 0 & +iJ & +ig\alpha_1^* & 0 \\ -iJ & 0 & -\left(\frac{\gamma_2}{2} + i\Delta_2\right) & 0 & 0 & 0 \\ 0 & +iJ & 0 & -\left(\frac{\gamma_2}{2} - i\Delta_2\right) & 0 & 0 \\ 0 & 0 & 0 & 0 & 0 & \omega_m \\ -g\alpha_1^* & -g\alpha_1 & 0 & 0 & -\omega_m & -\gamma_m \end{pmatrix} \quad (10)$$

with the effective detuning  $\Delta'_1 = \Delta_1 + g\bar{q}$ . The stability conditions for the system require that the real parts of all the eigenvalues of matrix  $A$  are negative, which can be given analytically by using the Routh-Hurwitz criterion [37–39]. However, the analytical conditions are too cumbersome to be given here. In the following, we will check the stability of the system by calculating the eigenvalues of matrix  $A$  numerically.

In this paper, we focus on the mean response of the system to the classical driving field. To discuss the difference of the mean response of the system to the classical driving field input from different optical modes, we will show the equations of the output fields when a classical field input from the optical mode  $a_1$  by setting  $\alpha_{1,\text{in}} = s_{\text{in}}$  and  $\alpha_{2,\text{in}} = 0$ , or input from the optical mode  $a_2$  by setting  $\alpha_{1,\text{in}} = 0$  and  $\alpha_{2,\text{in}} = s_{\text{in}}$ , respectively. Here,  $s_{\text{in}} = \sqrt{p_{\text{in}}/(\hbar\omega_d)}$  is the amplitude of the driving field with pump power  $p_{\text{in}}$ .

For the case of the classical field input from the optical mode  $a_1$ , i.e.,  $\alpha_{1,\text{in}} = s_{\text{in}}$  and  $\alpha_{2,\text{in}} = 0$ , we will derive the equation for the output field  $\alpha_{2,\text{out}}$  from the optical mode  $a_2$ . Eqs. (6) and (7) are rewritten with  $\bar{q} = -g|\alpha_1|^2/\omega_m$  as

$$0 = -\left(\frac{\gamma_1}{2} + i\Delta_1\right)\alpha_1 - iU|\alpha_1|^2\alpha_1 - iJ\alpha_2 + \sqrt{\eta_1\gamma_1}s_{\text{in}}, \quad (11)$$

$$0 = -\left(\frac{\gamma_2}{2} + i\Delta_2\right)\alpha_2 - iJ\alpha_1, \quad (12)$$

where  $U \equiv -g^2/\omega_m$  is the nonlinear interaction induced by the optomechanical interaction. Using Eq. (12), one has

$$\alpha_2 = \frac{-i2J}{\gamma_2 + i2\Delta_2}\alpha_1. \quad (13)$$

Substituting it into the standard input-output relation [40]

$$\alpha_{2,\text{out}} = \sqrt{\eta_2\gamma_2}\alpha_2 = \frac{-i2J\sqrt{\eta_2\gamma_2}}{\gamma_2 + i2\Delta_2}\alpha_1, \quad (14)$$

and Eq. (11), the equation for the output field  $\alpha_{2,\text{out}}$  can be written as

$$0 = -\left(\frac{\Gamma}{2} + i\bar{\Delta}\right)\alpha_{2,\text{out}} - iU_{21}|\alpha_{2,\text{out}}|^2\alpha_{2,\text{out}} + \varepsilon_{\text{eff}} \quad (15)$$

with the effective damping rate  $\Gamma$ , detuning  $\bar{\Delta}$ , nonlinear interaction strength  $U_{21}$ , and driving amplitude  $\varepsilon_{\text{eff}}$  given by

$$\Gamma \equiv \gamma_1 + \frac{4\gamma_2J^2}{\gamma_2^2 + 4\Delta_2^2}, \quad (16)$$

$$\bar{\Delta} \equiv \Delta_1 - \frac{4J^2\Delta_2}{\gamma_2^2 + 4\Delta_2^2}, \quad (17)$$

$$U_{21} \equiv \frac{\gamma_2^2 + 4\Delta_2^2}{4\eta_2\gamma_2J^2}U, \quad (18)$$

$$\varepsilon_{\text{eff}} \equiv -\frac{i2J\sqrt{\eta_1\gamma_1\eta_2\gamma_2}}{\gamma_2 + i2\Delta_2}s_{\text{in}}. \quad (19)$$

When the classical field is input from the optical mode  $a_2$ , i.e.,  $\alpha_{1,\text{in}} = 0$  and  $\alpha_{2,\text{in}} = s_{\text{in}}$ , we will consider the output field  $\alpha_{1,\text{out}}$  from the optical mode  $a_1$ . In this case, Eqs. (6) and (7) are rewritten as

$$0 = -\left(\frac{\gamma_1}{2} + i\Delta_1\right)\alpha_1 - iU|\alpha_1|^2\alpha_1 - iJ\alpha_2, \quad (20)$$

$$0 = -\left(\frac{\gamma_2}{2} + i\Delta_2\right)\alpha_2 - iJ\alpha_1 + \sqrt{\eta_2\gamma_2}s_{\text{in}}. \quad (21)$$

From Eq. (21) one has

$$\alpha_2 = \frac{-i2J}{\gamma_2 + i2\Delta_2}\alpha_1 + \frac{2\sqrt{\eta_2\gamma_2}}{\gamma_2 + i2\Delta_2}s_{\text{in}}, \quad (22)$$

which together with Eq. (20) and the input-output relation [40]

$$\alpha_{1,\text{out}} = \sqrt{\eta_1\gamma_1}\alpha_1 \quad (23)$$

provide the following equation for the output field  $\alpha_{1,\text{out}}$  as

$$0 = -\left(\frac{\Gamma}{2} + i\bar{\Delta}\right)\alpha_{1,\text{out}} - iU_{12}|\alpha_{1,\text{out}}|^2\alpha_{1,\text{out}} + \varepsilon_{\text{eff}} \quad (24)$$

with the effective nonlinear interaction strength

$$U_{12} \equiv \frac{U}{\eta_1\gamma_1}. \quad (25)$$

In order to find the output field  $|\alpha_{i,\text{out}}|^2$  ( $i = 1, 2$ ), Eqs. (15) and (24) can be rewritten in a unified form as

$$\left(\frac{\Gamma^2}{4} + \bar{\Delta}^2\right)|\alpha_{i,\text{out}}|^2 + 2\bar{\Delta}U_{\text{eff}}|\alpha_{i,\text{out}}|^4 + U_{\text{eff}}^2|\alpha_{i,\text{out}}|^6 = |\varepsilon_{\text{eff}}|^2, \quad (26)$$

where  $U_{\text{eff}} = U_{12}$  for  $|\alpha_{1,\text{out}}|^2$  and  $U_{\text{eff}} = U_{21}$  for  $|\alpha_{2,\text{out}}|^2$ . The output field  $|\alpha_{i,\text{out}}|^2$  is found to have three possible real

values, the so-called optical bistability, under some conditions. One way to get the bistability condition is to take a derivative of Eq. (26) with respect to  $|\alpha_{i,\text{out}}|^2$ , then we have

$$\left(\frac{\Gamma^2}{4} + \bar{\Delta}^2\right) + 4\bar{\Delta}U_{\text{eff}}|\alpha_{i,\text{out}}|^2 + 3U_{\text{eff}}^2|\alpha_{i,\text{out}}|^4 = 0. \quad (27)$$

Thus the value of  $|\alpha_{i,\text{out}}|^2$  corresponding to the bistability turning point is the two roots of the above equation,

$$|\alpha_{i,\text{out}}|_{\pm}^2 = \frac{-4\bar{\Delta} \mp \sqrt{4\bar{\Delta}^2 - 3\Gamma^2}}{6U_{\text{eff}}} > 0 \quad (28)$$

with the bistability condition (positive values of the discriminant)

$$\bar{\Delta} > \frac{\sqrt{3}}{2}\Gamma. \quad (29)$$

It is well known that the intermediate value in the bistability region is unstable for it corresponds to the maximum (not minimum) point in the effective potential energy. Different from the Kerr medium, where the upper and lower values are always stable, the other type of instability may appear in the upper value of an optomechanical system due to the heating of the mechanical mode, which may result in the negative effective damping of the mechanical mode in the blue-detuned regime or strong driving condition [41–45].

The transmission coefficient in the direction from the optical mode  $a_1$  to the optical mode  $a_2$  is defined by

$$T_{21} \equiv \left| \frac{\alpha_{2,\text{out}}}{\alpha_{1,\text{in}}} \right|^2, \quad (30)$$

and the transmission coefficient in the opposite direction is defined by

$$T_{12} \equiv \left| \frac{\alpha_{1,\text{out}}}{\alpha_{2,\text{in}}} \right|^2. \quad (31)$$

The efficiency for the nonreciprocity transmission can be described by the isolation

$$I = \frac{T_{21}}{T_{12}}. \quad (32)$$

From the nonlinear equations for  $\alpha_{2,\text{out}}$  [Eq. (15)] and  $\alpha_{1,\text{out}}$  [Eq. (24)], it is interesting to note that, when

$$\sqrt{\eta_1\gamma_1} = \left| \frac{-i2J}{\gamma_2 + i2\Delta_2} \right| \sqrt{\eta_2\gamma_2}, \quad (33)$$

the reciprocity will be observed for  $U_{21} = U_{12}$ , even when  $U_{21} \neq 0$ .  $\sqrt{\eta_1\gamma_1}$  is the coupling rate of the optical mode  $a_{1,\text{in}}$  to  $a_1$ , and  $|-i2J/(\gamma_2 + i2\Delta_2)|\sqrt{\eta_2\gamma_2}$  is the effective coupling rate of the optical mode  $a_1$  to  $a_{2,\text{out}}$  through the optical mode  $a_2$  [see Eq. (14)]. We refer to Eq. (33) as the impedance-matching condition for these two coupling rates are equal. On the contrary, if the impedance-matching condition is broken,

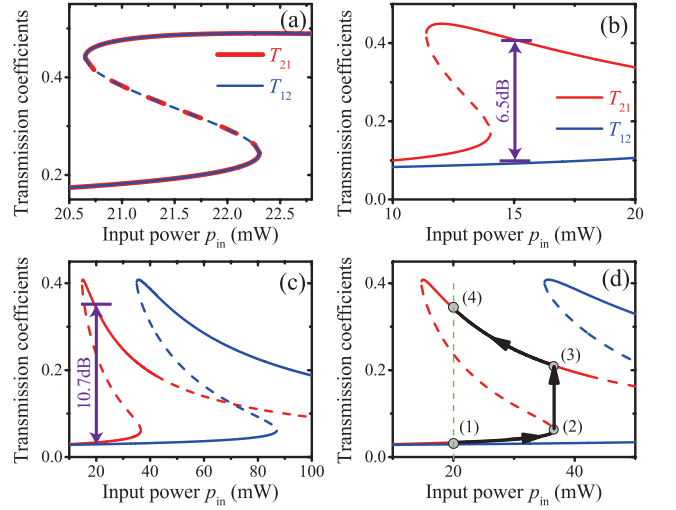


FIG. 2: (Color online) Transmission coefficients  $T_{21}$  (red) and  $T_{12}$  (blue) as a function of the input power  $p_{\text{in}}$  (mW). (a)  $\Delta_1/2\pi = 2$  GHz,  $\Delta_2 = 0$ ,  $J/2\pi = 0.5$  GHz; (b)  $\Delta_1/2\pi = \Delta_2/2\pi = 4$  GHz,  $J/2\pi = 3$  GHz; (c) and (d)  $\Delta_1/2\pi = \Delta_2/2\pi = 4.6$  GHz,  $J/2\pi = 3$  GHz. The dashed curves correspond to the unstable regimes for the eigenvalues of the matrix  $A$  containing positive real parts. The other parameters are  $\omega_d/2\pi = 200$  THz,  $\gamma_1/2\pi = \gamma_2/2\pi = 1$  GHz,  $\eta_1 = \eta_2 = 0.7$ ,  $\omega_m/2\pi = 6$  GHz,  $\gamma_m/2\pi = 5$  MHz, and  $g/2\pi = 0.8$  MHz.

we will have  $U_{21} \neq U_{12}$ , i.e., the effective nonlinearity induced by the optomechanical interaction is different for photons transport in different directions, and as a result the optical nonreciprocity appears in the three-mode optomechanical system, i.e.,  $T_{21} \neq T_{12}$ . That is to say nonlinearity is a necessary but not a sufficient condition for observing nonreciprocity, and breaking the impedance-matching condition is another necessary condition for nonreciprocal response of the system.

### III. NONRECIPROCAL TRANSMISSION

In this section, we will discuss the effects of the parameters on the nonreciprocal transmission of light input from different optical modes by solving the equations numerically. For numerical simulation, we use parameters based on a recent experiment on the observation of nonreciprocity in an optomechanical crystal [25]:  $\omega_d/2\pi \approx 200$  THz,  $\gamma_1/2\pi = \gamma_2/2\pi = 1$  GHz,  $\eta_1 = \eta_2 = 0.7$ ,  $\omega_m/2\pi = 6$  GHz,  $\gamma_m/2\pi = 5$  MHz, and  $g/2\pi = 0.8$  MHz.

In Fig. 2, we show the transmission coefficients  $T_{21}$  (red) and  $T_{12}$  (blue) as a function of the input power  $p_{\text{in}}$ . First of all, let us check the necessary condition for nonreciprocity numerically. Although the system works in the bistable regime, as shown in Fig. 2(a), the nonreciprocity can not be observed, i.e.,  $T_{12} = T_{21}$ , when the impedance-matching condition given by Eq. (33) is satisfied. Conversely, the nonreciprocity appears when the impedance-matching condition is broken, as shown in Fig. 2(b). The related isolation is  $I \approx 6.5$  dB for input power  $p_{\text{in}} = 15$  mW, with the detunings  $\Delta_1/2\pi =$



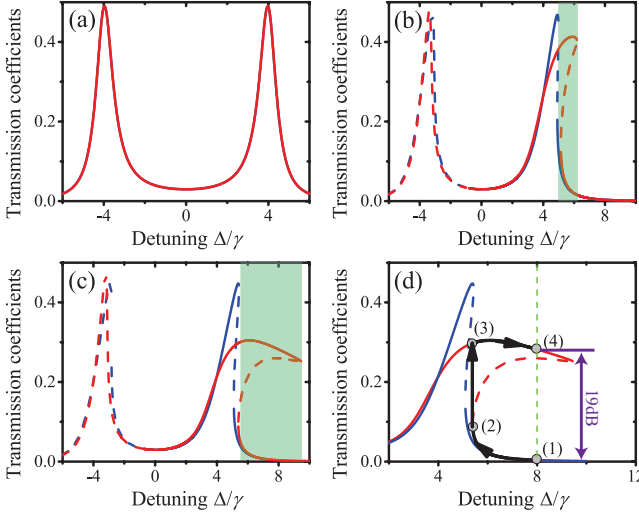


FIG. 3: (Color online) Transmission coefficients  $T_{21}$  (red) and  $T_{12}$  (blue) as a function of the detuning  $\Delta/\gamma$  ( $\Delta \equiv \Delta_1 = \Delta_2$ ,  $\gamma \equiv \gamma_1 = \gamma_2$ ). (a)  $p_{\text{in}} = 0.1$  mW; (b)  $p_{\text{in}} = 20$  mW; (c) and (d)  $p_{\text{in}} = 30$  mW. The other parameters are  $\omega_d/2\pi \approx 200$  THz,  $\gamma_1/2\pi = \gamma_2/2\pi = 1$  GHz,  $J/2\pi = 4$  GHz,  $\eta_1 = \eta_2 = 0.7$ ,  $\omega_m/2\pi = 6$  GHz,  $\gamma_m/2\pi = 5$  MHz, and  $g/2\pi = 0.8$  MHz. The region for notable nonreciprocity is marked out with green colour.

$\Delta_2/2\pi = 4$  GHz and coupling strength  $J/2\pi = 3$  GHz. The isolation can be improved to be  $I \approx 10.7$  dB for input power  $p_{\text{in}} = 20$  mW when the detunings  $\Delta_1/2\pi = \Delta_2/2\pi = 4.6$  GHz, as shown in Fig. 2(c). In order to make the system work in the upper branch, see Fig. 2(d), we can increase the input power (1) to the critical power (2) [or (3)] for optical bistability, and then reduce the input power to the working power in the upper branch (4).

We note that it is possible to achieve optical isolation with high transmission in the direction from  $a_2$  to  $a_1$ , as shown in Fig. 2(c) around  $p_{\text{in}} = 40$  mW. However, the isolation in this direction is much lower than the isolation can be achieved in the opposite direction. Moreover, the require power is much higher, and worse yet, the high power with  $p_{\text{in}} > 44$  mW will cause instability for field input from  $a_1$ , as shown in Fig. 2(c). So we only consider the optical isolation with high transmission from  $a_1$  to  $a_2$  in the following.

The transmission coefficients  $T_{21}$  (red) and  $T_{12}$  (blue) plotted as a function of the detuning  $\Delta/\gamma$  ( $\Delta \equiv \Delta_1 = \Delta_2$ ,  $\gamma \equiv \gamma_1 = \gamma_2$ ) are shown in Fig. 3 for different input powers. When the input power is low, e.g.,  $p_{\text{in}} = 0.1$  mW, there are peaks around the two resonant frequencies with the detuning  $\Delta \approx \pm J$ , and the nonreciprocity effect is not pronounced. As the input power increases, the optical bistability occurs and the nonreciprocity effect becomes visible with the detuning  $\Delta > J$  [see Figs. 3(b) and 3(c)]. In order to make the system work in the upper branch, see Fig. 3(d), we can tune the frequency of the input field from (1) to the critical detuning (2) [or (3)] for the optical bistability, and then increase the frequency of the input field to the working frequency in the upper branch (4). In the case with  $\Delta = 2J$ ,  $p_{\text{in}} = 30$  mW, and  $J = 2\pi \times 6$  GHz, the system can work with the transmission

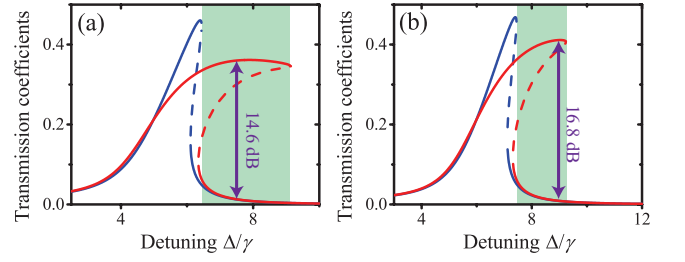


FIG. 4: (Color online) Transmission coefficients  $T_{21}$  (red) and  $T_{12}$  (blue) as a function of the detuning  $\Delta/\gamma$  ( $\Delta \equiv \Delta_1 = \Delta_2$ ,  $\gamma \equiv \gamma_1 = \gamma_2$ ). (a)  $J/2\pi = 5$  GHz; (b)  $J/2\pi = 6$  GHz. The other parameters are  $\omega_d/2\pi \approx 200$  THz,  $\gamma_1/2\pi = \gamma_2/2\pi = 1$  GHz,  $p_{\text{in}} = 30$  mW,  $\eta_1 = \eta_2 = 0.7$ ,  $\omega_m/2\pi = 6$  GHz,  $\gamma_m/2\pi = 5$  MHz, and  $g/2\pi = 0.8$  MHz. The region for notable nonreciprocity is marked out with green colour.

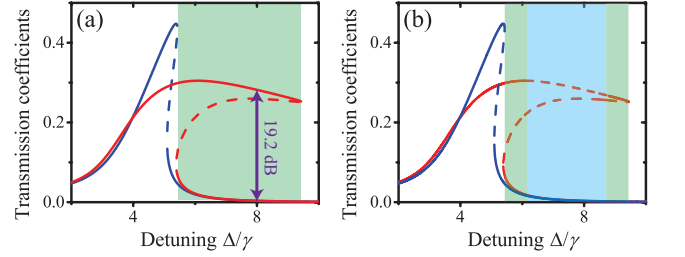


FIG. 5: (Color online) Transmission coefficients  $T_{21}$  (red) and  $T_{12}$  (blue) as a function of the detuning  $\Delta/\gamma$  ( $\Delta \equiv \Delta_1 = \Delta_2$ ,  $\gamma \equiv \gamma_1 = \gamma_2$ ). (a)  $\omega_m/2\pi = 6$  GHz,  $g/2\pi = 8$  MHz and  $p_{\text{in}} = 0.3$  mW; (b)  $\omega_m/2\pi = 6/1.1$  GHz,  $g/2\pi = 0.8$  MHz and  $p_{\text{in}} = 30/1.1$  mW. The other parameters are  $\omega_d/2\pi \approx 200$  THz,  $\gamma_1/2\pi = \gamma_2/2\pi = 1$  GHz,  $J/2\pi = 4$  GHz,  $\eta_1 = \eta_2 = 0.7$ , and  $\gamma_m/2\pi = 5$  MHz. The region for notable nonreciprocity is marked out with green colour, and the region for unstable upper branch is marked out with blue colour.

coefficients  $T_{21} \approx 0.28$ ,  $T_{12} \approx 0.00335$ , and the isolation  $I \approx 19$  dB.

It is worth mentioning that the optical multiple solutions may also occur with the detuning satisfying  $-J < \Delta < 0$ , but the system is unstable in this regime, which are shown by dashed curves in Figs. 3(b) and 3(c). This instability is induced by the heating of the mechanical mode in the blue-detuned regime  $\Delta < 0$ , for the effective damping of the mechanical mode may become negative [41–45].

Different from the behavior of bistability in a standard optomechanical system with one mechanical mode coupled to one optical mode [45], the peaks “arch down” as a function of detuning, as shown in Fig. 3(c). This phenomenon is induced by the detuning-dependent nonlinear interaction strength  $U_{21}$  in Eq. (18). More specifically, the nonlinear interaction strength  $U_{21}$  increases with increasing detuning, and the transmission coefficient  $T_{21}$  is suppressed by the increasing nonlinear interaction strength  $U_{21}$  with increasing detuning. By contrast, there is no such suppression in  $T_{12}$  for the constant nonlinear interaction strength  $U_{12}$  in Eq. (25).

Now we will discuss the ideal range of parameters for no-

table nonreciprocity with high transmission coefficients. Figure 4 presents the transmission coefficients  $T_{21}$  (red) and  $T_{12}$  (blue) as a function of the detuning  $\Delta/\gamma$  for different coupling strength  $J$ . It is clear that both the isolation  $I$  and the transmission coefficient  $T_{21}$  are improved with a larger coupling strength  $J$ . However, the frequency range for the nonreciprocity (marked out with green colour) becomes narrower. In some experiments [46, 47], the coupling strength  $J$  between the two optical cavities is tunable by adjusting the gap between two cavities.

The optomechanical coupling strength  $g$  and the frequency of the mechanical mode  $\omega_m$  are two critical parameters in optomechanical systems for the nonlinear interaction strength  $U = -g^2/\omega_m$ . The nonlinear interaction strength  $U$  can be enhanced with a stronger optomechanical coupling strength  $g$  or lower mechanical frequency  $\omega_m$ . As shown in Fig. 5(a), if  $g$  is enhanced by one order of magnitude, the input power will be reduced by two orders of magnitude. That means the optomechanically induced nonreciprocity can be achieved with a much lower input power if the coupling strength  $g$  can be enhanced in experiments.

As shown in Fig. 5(b), the input power for realizing optomechanically induced nonreciprocity can also be reduced with lower mechanical frequency  $\omega_m$ . However, the upper branch becomes unstable (marked out with blue colour) due to the position fluctuations of the mechanical mode for the effective damping of the mechanical mode may become negative [41–45]. The unstable upper branch will also appear in the case of lower mechanical frequency  $\omega_m/k$  and smaller optomechanical coupling strength  $g/\sqrt{k}$  ( $k > 1$ ), with the nonlinear interaction strength  $U = -g^2/\omega_m$  unchanged. Therefore, mechanical modes of high frequency are conducive to the stability of the systems.

## IV. CONCLUSIONS

In summary, we have shown that the three-mode optomechanical system can be used to realize the nonreciprocity for a strong light beam injected into the system, due to the existence of the optomechanical nonlinearity. The nonlinearity is a necessary, but not a sufficient condition for observing nonreciprocal transport. Breaking of impedance-matching condition is another pivotal condition for nonreciprocity. By adjusting the tunable parameters, we can realize the nonreciprocity with both high isolation and high transmission coefficients in the allowed transmission direction. Our work paves the way towards the nonreciprocal transmission for strong optical signals in optomechanical systems. There are still two points that need be specified because they may restrict the applications of our proposal in some fields. First, the optical isolation is highly sensitive to given parameters and particularly to the power of the propagating light. Secondly, if system works under bistable conditions, it has to be initialized by varying the detuning or the strength every time that the optical isolation is required. Therefore how to overcome these issues or even use them for useful applications need to be further studied in the future.

### Acknowledgement

We thank Dr. Cheng Jiang for helpful discussions. X.W.X. was supported by the National Natural Science Foundation of China (NSFC) under Grant No. 11604096. Z.H.W. was supported by the NSFC under Grant No. 11875011. Y.L. acknowledges the support from the NSFC under Grant No. 11774024, No. 11534002, and No. U1530401.

- 
- [1] T. J. Kippenberg and K. J. Vahala, Cavity Optomechanics: Back-Action at the Mesoscale, *Science* **321**, 1172 (2008).
  - [2] F. Marquardt and S. M. Girvin, Optomechanics, *Physics* **2**, 40 (2009).
  - [3] M. Aspelmeyer, P. Meystre, and K. Schwab, Quantum optomechanics, *Phys. Today* **65**(7), 29 (2012).
  - [4] M. Aspelmeyer, T. J. Kippenberg, and F. Marquardt, Cavity Optomechanics, *Rev. Mod. Phys.* **86**, 1391 (2014).
  - [5] M. Metcalfe, Applications of cavity optomechanics, *Appl. Phys. Rev.* **1**, 031105 (2014).
  - [6] Y. L. Liu, C. Wang, J. Zhang, and Y. X. Liu, Cavity optomechanics: Manipulating photons and phonons towards the single-photon strong coupling, *Chin. Phys. B* **27**, 024204 (2018).
  - [7] E. Verhagen and A. Alù, Optomechanical nonreciprocity, *Nat. Phys.* **13**, 922 (2017).
  - [8] D. L. Sounas, and A. Alù, Non-reciprocal photonics based on time modulation, *Nat. Photonics* **11**, 774 (2017).
  - [9] G. S. Agarwal and S. Huang, Electromagnetically induced transparency in mechanical effects of light, *Phys. Rev. A* **81**, 041803(R) (2010).
  - [10] S. Weis, R. Rivière, S. Deléglise, E. Gavartin, O. Arcizet, A. Schliesser, and T. J. Kippenberg, Optomechanically Induced Transparency, *Science* **330**, 1520 (2010).
  - [11] Q. Lin, J. Rosenberg, D. Chang, R. Camacho, M. Eichenfield, K. J. Vahala, and O. Painter, Coherent mixing of mechanical excitations in nano-optomechanical structures, *Nat. Photonics* **4**, 236 (2010).
  - [12] A. H. Safavi-Naeini, T. P. M. Alegre, J. Chan, M. Eichenfield, M. Winger, Q. Lin, J. T. Hill, D. Chang, and O. Painter, Electromagnetically induced transparency and slow light with optomechanics, *Nature (London)* **472**, 69 (2011).
  - [13] J. D. Teufel, D. Li, M. S. Allman, K. Cicak, A. J. Sirois, J. D. Whittaker, and R. W. Simmonds, Circuit cavity electromechanics in the strong-coupling regime, *Nature (London)* **471**, 204 (2011).
  - [14] M. Hafezi and P. Rabl, Optomechanically induced nonreciprocity in microring resonators, *Opt. Express* **20**, 7672 (2012).
  - [15] Z. Shen, Y. L. Zhang, Y. Chen, C. L. Zou, Y. F. Xiao, X. B. Zou, F. W. Sun, G. C. Guo, and C. H. Dong, Experimental realization of optomechanically induced non-reciprocity, *Nat. Photonics* **10**, 657 (2016).
  - [16] F. Ruesink, M.-A. Miri, A. Alù, and E. Verhagen, Nonreciprocity and magnetic-free isolation based on optomechanical interactions, *Nat. Commun.* **7**, 13662 (2016).
  - [17] C. H. Dong, Z. Shen, C. L. Zou, Y. L. Zhang, W. Fu, and G. C. Guo, Brillouin-scattering-induced transparency and nonre-

- ciprocal light storage, *Nat. Commun.* **6**, 6193 (2015).
- [18] J. Kim, M. C. Kuzyk, K. Han, H. Wang, and G. Bahl, Nonreciprocal Brillouin scattering induced transparency, *Nature Phys.* **11**, 275 (2015).
- [19] X. W. Xu and Y. Li, Optical nonreciprocity and optomechanical circulator in three-mode optomechanical systems, *Phys. Rev. A* **91**, 053854 (2015).
- [20] A. Metelmann and A. A. Clerk, Nonreciprocal Photon Transmission and Amplification via Reservoir Engineering, *Phys. Rev. X* **5**, 021025 (2015).
- [21] X. W. Xu, Y. Li, A. X. Chen, and Y. X. Liu, Nonreciprocal conversion between microwave and optical photons in electro-optomechanical systems, *Phys. Rev. A* **93**, 023827 (2016).
- [22] L. Tian and Z. Li, Nonreciprocal quantum-state conversion between microwave and optical photons, *Phys. Rev. A* **96**, 013808 (2017).
- [23] G. Li, X. Xiao, Y. Li, and X. G. Wang, Tunable optical nonreciprocity and a phonon-photon router in an optomechanical system with coupled mechanical and optical modes, *Phys. Rev. A* **97**, 023801 (2018).
- [24] C. Jiang, L. N. Song, and Y. Li, Directional amplifier in an optomechanical system with optical gain, *Phys. Rev. A* **97**, 053812 (2018).
- [25] K. Fang, J. Luo, A. Metelmann, M. H. Matheny, F. Marquardt, A. A. Clerk, and O. Painter, Generalized non-reciprocity in an optomechanical circuit via synthetic magnetism and reservoir engineering, *Nat. Phys.* **13**, 465 (2017).
- [26] G. A. Peterson, F. Lecocq, K. Cicak, R. W. Simmonds, J. Aumentado, and J. D. Teufel, Demonstration of Efficient Nonreciprocity in a Microwave Optomechanical Circuit, *Phys. Rev. X* **7**, 031001 (2017).
- [27] N. R. Bernier, L. D. Toth, A. Koottandavida, M. Ioannou, D. Malz, A. Nunnenkamp, A. K. Feofanov, and T. J. Kippenberg, Nonreciprocal reconfigurable microwave optomechanical circuit, *Nat. Commun.* **8**, 604 (2017).
- [28] S. Barzanjeh, M. Wulf, M. Peruzzo, M. Kalae, P. B. Dieterle, O. Painter, and J. M. Fink, Mechanical On-Chip Microwave Circulator, *Nat. Commun.* **8**, 953 (2017).
- [29] S. Manipatruni, J. T. Robinson, and M. Lipson, Optical Nonreciprocity in Optomechanical Structures, *Phys. Rev. Lett.* **102**, 213903 (2009).
- [30] Z. Wang, L. Shi, Y. Liu, X. Xu, and X. Zhang, Optical Nonreciprocity in Asymmetric Optomechanical Couplers. *Sci. Rep.* **5**, 8657 (2015).
- [31] H. Qiu, J. Dong, L. Liu, and X. Zhang, Energy-efficient on-chip optical diode based on the optomechanical effect, *Opt. Express* **25**, 8975 (2017).
- [32] T. K. Paraíso, M. Kalae, L. Zang, H. Pfeifer, F. Marquardt, and O. Painter, Position-Squared Coupling in a Tunable Photonic Crystal Optomechanical Cavity, *Phys. Rev. X* **5**, 041024 (2015).
- [33] N. E. Flowers-Jacobs, S. W. Hoch, J. C. Sankey, A. Kashkanova, A. M. Jayich, C. Deutsch, J. Reichel, and J. G. E. Harris, Fiber-Cavity-Based Optomechanical Device, *Appl. Phys. Lett.* **101**, 221109 (2012).
- [34] J. D. Thompson, B. M. Zwickl, A. M. Jayich, F. Marquardt, S. M. Girvin, and J. G. E. Harris, Strong dispersive coupling of a high-finesse cavity to a micromechanical membrane, *Nature (London)* **452**, 72 (2008).
- [35] H. Xu, D. Mason, L. Jiang, and J. G. E. Harris, Topological energy transfer in an optomechanical system with exceptional points, *Nature (London)* **537**, 80 (2016).
- [36] H. Xu, U. Kemiktarak, J. Fan, S. Ragole, J. Lawall, and J. M. Taylor, Observation of optomechanical buckling transitions, *Nat. Commun.* **8**, 14481 (2017).
- [37] E. X. DeJesus and C. Kaufman, Routh-Hurwitz criterion in the examination of eigenvalues of a system of nonlinear ordinary differential equations, *Phys. Rev. A* **35**, 5288 (1987).
- [38] I. S. Gradshteyn and I. M. Ryzhik, in *Table of Integrals, Series and Products* (Academic, Orlando, 1980), p. 1119.
- [39] M. Paternostro, S. Gigan, M. S. Kim, F. Blaser, H. R. Böhm, and M. Aspelmeyer, Reconstructing the dynamics of a movable mirror in a detuned optical cavity, *New J. Phys.* **8**, 107 (2006).
- [40] C. W. Gardiner and M. J. Collett, Input and output in damped quantum systems: Quantum stochastic differential equations and the master equation, *Phys. Rev. A* **31**, 3761 (1985).
- [41] T. Carmon, H. Rokhsari, L. Yang, T. J. Kippenberg, and K. J. Vahala, Temporal Behavior of Radiation-Pressure-Induced Vibrations of an Optical Microcavity Phonon Mode, *Phys. Rev. Lett.* **94**, 223902 (2005).
- [42] T. J. Kippenberg, H. Rokhsari, T. Carmon, A. Scherer, and K. J. Vahala, Analysis of Radiation-Pressure Induced Mechanical Oscillation of an Optical Microcavity, *Phys. Rev. Lett.* **95**, 033901 (2005).
- [43] F. Marquardt, J. G. E. Harris, and S. M. Girvin, Dynamical Multistability Induced by Radiation Pressure in High-Finesse Micromechanical Optical Cavities, *Phys. Rev. Lett.* **96**, 103901 (2006).
- [44] M. Ludwig, B. Kubala and F. Marquardt, The optomechanical instability in the quantum regime, *New J. Phys.* **10**, 095013 (2008).
- [45] S. Aldana, C. Bruder, and A. Nunnenkamp, Equivalence between an optomechanical system and a Kerr medium, *Phys. Rev. A* **88**, 043826 (2013).
- [46] B. Peng, S. K. Ozdemir, F. C. Lei, F. Monifi, M. Gianfreda, G. L. Long, S. H. Fan, F. Nori, C. M. Bender, and L. Yang, Parity-time-symmetric whispering-gallery microcavities, *Nat. Phys.* **10**, 394 (2014).
- [47] L. Chang, X. S. Jiang, S. Y. Hua, C. Yang, J. M. Wen, L. Jiang, G. Y. Li, G. Z. Wang, and M. Xiao, Parity-time symmetry and variable optical isolation in active-passive-coupled microresonators, *Nat. Photonics* **8**, 524 (2014).